PROCEEDINGS OF SPIE

Fifteenth International Conference on Correlation Optics

Oleg V. Angelsky
Editor

13–16 September 2021
Chernivtsi, Ukraine

Organized by
Chernivtsi National University (Ukraine)

Co-organized by
Research Institute of Zhejiang University-Taizhou (China)

Sponsored by
ICO – International Commission for Optics
Optica (formerly OSA), the Society Advancing Optics and Photonics Worldwide
Frontiers in Physics LTD
LTD "ROMA"
SKB "ELEKTRONMASH" (Ukraine)
Private Clinic of Eye Microsurgery "Your Vision" (Ukraine)
ARTON Company (Ukraine)

Co-sponsored by
SPIE

Published by
SPIE

Volume 12126

Proceedings of SPIE 0277-786X, V. 12126

SPIE is an international society advancing an interdisciplinary approach to the science and application of light.

Fifteenth International Conference on Correlation Optics, edited by Oleg V. Angelsky, Proc. of SPIE Vol. 12126, 1212601
 · 0277-786X · doi: 10.1117/12.2626737

The papers in this volume were part of the technical conference cited on the cover and title page. Papers were selected and subject to review by the editors and conference program committee. Some conference presentations may not be available for publication. Additional papers and presentation recordings may be available online in the SPIE Digital Library at SPIEDigitalLibrary.org.

The papers reflect the work and thoughts of the authors and are published herein as submitted. The publisher is not responsible for the validity of the information or for any outcomes resulting from reliance thereon.

Please use the following format to cite material from these proceedings:
Author(s), "Title of Paper," in *Fifteenth International Conference on Correlation Optics*, edited by Oleg V. Angelsky, Proc. of SPIE 12126, Seven-digit Article CID Number (DD/MM/YYYY); (DOI URL).

ISSN: 0277-786X
ISSN: 1996-756X (electronic)

ISBN: 9781510651289
ISBN: 9781510651296 (electronic)

Published by
SPIE
P.O. Box 10, Bellingham, Washington 98227-0010 USA
Telephone +1 360 676 3290 (Pacific Time)
SPIE.org

Printed in the United States of America by Curran Associates, Inc., under license from SPIE.

Publication of record for individual papers is online in the SPIE Digital Library.

SPIE. DIGITAL LIBRARY
SPIEDigitalLibrary.org

Paper Numbering: A unique citation identifier (CID) number is assigned to each article in the Proceedings of SPIE at the time of publication. Utilization of CIDs allows articles to be fully citable as soon as they are published online, and connects the same identifier to all online and print versions of the publication. SPIE uses a seven-digit CID article numbering system structured as follows:

- The first five digits correspond to the SPIE volume number.
- The last two digits indicate publication order within the volume using a Base 36 numbering system employing both numerals and letters. These two-number sets start with 00, 01, 02, 03, 04, 05, 06, 07, 08, 09, 0A, 0B … 0Z, followed by 10-1Z, 20-2Z, etc. The CID Number appears on each page of the manuscript.

Mueller-matrix microscopy of laser-induced monochromatic fluorescent fields of preparations of human internal organs and histological diagnostics of the time of age of damage formation

Litvinenko[1] A.Yu., Kvasnyuk[1] D., Vanchulyak[1] A.Ya., Stashkevich[2] M., Motrich[3] A.V., Mikhailova[3] A.Yu., Gorskiy[3] M.P., Slyotov[3] M.M.
[1]Bukovinian State Medical University, Chernivtsi, Ukraine
[2]The Institute of Traumatology and Orthopedics by NAMS of Ukraine, Kyiv, Ukraine
[3] Chernivtsi National University, Chernivtsi, Ukraine
m.gorskii@chnu.edu.ua

ABSTRACT

The article contains the results of experimental testing of methods of azimuthal-invariant Mueller-matrix microscopy (Mueller-matrix invariants - MMI) of optically anisotropic fluorophores of samples of histological sections of the brain, liver and kidney, as well as myocardium and lung tissue; temporal detection of variations in the magnitude of the statistical moments of the 1st - 4th orders, characterizing the distributions of the MMI value of linear birefringence and optical activity of samples of histological sections of the brain, liver and kidney, as well as myocardium and lung tissue with different age of damage; determination of the diagnostic efficiency (time interval and accuracy) of establishing the age of damage to human internal organs by digital histological methods of MMI mapping of optical anisotropy of fluorophores in histological sections of the brain, liver and kidney, as well as myocardium and lung tissue.

Keywords: polarization, Mueller matrix, linear birefringence, statistical moments of the 1st - 4th orders, histological sections, biological tissues, damages

1. INTRODUCTION

Methods and means of Mueller-matrix polarimetry [1-5] of biological tissues and fluids of human organs are described in detail in many works of groups of domestic (Dubolazov A.V., Ushenko Yu.) [6-15] and foreign (N. Gosh, A. Vitkin, Tuchin V. V. and others) scientists [16-19].

However, at present, these digital methods of polarizing Mueller-matrix microscopy are practically absent in histological studies of determining the age of damage to human internal organs. In addition, the analysis of microscopic images is performed semi-qualitatively by observing the structure of the image by an expert, followed by his subjective conclusion.

The aim of the study is to develop a set of objective forensic criteria for establishing the age of damage to human internal organs according to the data of the azimuthal-invariant Mueller matrix mapping of the polycrystalline structure of molecular domains-fluorophores of prototypes.

2. MATERIALS AND METHODS

The following groups were formed (control for those who died from coronary artery disease and experienced with different age of damage) of prototypes of histological sections of internal organs (brain, liver, kidney, as well as the myocardium and lung tissue) of a person [20-26].

Fifteenth International Conference on Correlation Optics, edited by Oleg V. Angelsky, Proc. of SPIE Vol. 12126, 1212623
 · 0277-786X · doi: 10.1117/12.2616667

Internal organ Brain, Liver, Kidney, Myocardium, Lung tissue	Groups									
	Control	Experienced with different age of damage, hours								
	Deceased from CAD(21)	1	6	12	18	24	48	72	96	120
		21	21	21	21	21	21	21	21	21

The study design consisted of the fact that within each of the groups of samples:

- obtained MMI maps of linear and circular birefringence of molecular fluorophores;
- the statistical moments of the 1st - 4th orders were calculated, characterizing the distributions of the value of the set of MMI;
- was determined within the control and the set of research groups, the average value and the error of the magnitude of each of the statistical moments of the 1st - 4th orders;
- the age of the damage and its accuracy were calculated algorithmically.

3. DIFFERENTIAL HISTOLOGICAL DIAGNOSTICS OF THE AGE OF FORMATION OF INJURIES OF HUMAN INTERNAL ORGANS BY MAPPING THE MULLER-MATRIX INVARIANT OF LINEAR BIREFRINGENCE

Coordinate ((1) – (3)) and statistical ((4) – (6)) structure of MMI of linear birefringence of histological sections of the brain with research ((1), (4)) and two control ((2), (3) (5), (6)) groups is shown in Fig. 1.

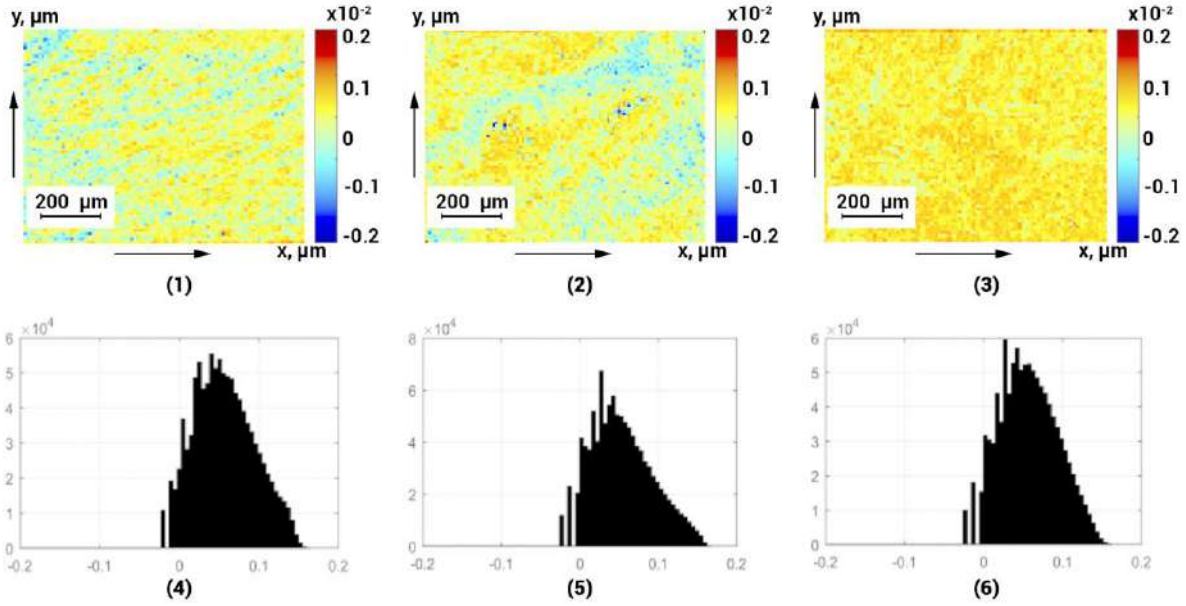

Fig. 1. Maps ((1), (2), (3)) and histograms ((4), (5), (6)) of the distributions of the MMI value of linear birefringence (x4) of histological sections of the brain of the deceased from the control group ((1), (4)), research groups with different duration of damage (6 hours - (2), (5)) and (18 hours - (3), (6)).

Mueller matrix microscopy of histological sections of the brain revealed:

- coordinate heterogeneity of all MMI maps, - fragments ((1) - (3));
- the presence of a significant scatter of MMI values in the corresponding histograms of distributions for different age of damage, - fragments ((4) - (6));
- a decrease in the level of crystallization of the brain substance with an increase in the age of damage - the average value and dispersion of the distributions of the MMI value of linear birefringence, calculated for the prescription of damage of 6 hours, decrease. (Fragment (5)) and 18 hours (Fragment (6)).

Quantitatively, the temporal transformation of the magnitude of the statistical moments of the 1st - 4th orders characterizing the distributions of the MMI of linear birefringence (4x) of brain samples is given in Table 1..

Analysis of the temporal dynamics of changes in the magnitude of the statistical moments, which are presented in Table 1, revealed diagnostic efficiency at a certain age of damage to internal organs of the following parameters:

- statistical moment of the 2nd order - the interval of linear and statistically significant ($p \prec 0{,}05$) change 6 hours with a dynamic range of 0.11;
- skewness and kurtosis - the duration of the linear interval up to 18 hours with a dynamic range of 0.84 and 0.72, respectively;

The greater diagnostic sensitivity of the Mueller-matrix microscopy technique was ensured by the use of large-scale (40x) polarization mapping of the degree of crystallization of histological sections of the brain of the control and a set of research samples of samples, - Fig. 2, table 2.

Table 1 Time dynamics of changes in statistical moments of the 1st - 4th orders, characterizing the distribution of MMI LB

T, hours	**2**	**4**	**6**	**12**	**18**
SM_1 x10^{-1}	$0{,}42 \pm 0{,}027$	$0{,}39 \pm 0{,}023$	$0{,}37 \pm 0{,}016$	$0{,}35 \pm 0{,}015$	$0{,}33 \pm 0{,}014$
p	$p \succ 0{,}05$				
SM_2 x10^{-1}	$0{,}94 \pm 0{,}041$	$0{,}83 \pm 0{,}038$	$0{,}79 \pm 0{,}036$	$0{,}74 \pm 0{,}034$	$0{,}71 \pm 0{,}035$
p	$p \prec 0{,}05$		$p \succ 0{,}05$		
SM_3	$0{,}39 \pm 0{,}019$	$0{,}53 \pm 0{,}028$	$0{,}67 \pm 0{,}031$	$0{,}95 \pm 0{,}042$	$1{,}23 \pm 0{,}058$
p	$p \prec 0{,}05$				
SM_4	$0{,}16 \pm 0{,}08$	$0{,}27 \pm 0{,}013$	$0{,}38 \pm 0{,}016$	$0{,}62 \pm 0{,}032$	$0{,}88 \pm 0{,}041$
p	$p \prec 0{,}05$				
T, hours	**24**	**48**	**72**	**96**	**120**
SM_1 x10^{-1}	$0.36 \pm 0{,}019$	$0{,}34 \pm 0{,}018$	$0{,}32 \pm 0{,}017$	$0{,}33 \pm 0{,}018$	$0{,}32 \pm 0{,}017$
p	$p \succ 0{,}05$				
SM_2 x10^{-1}	$0{,}68 \pm 0{,}035$	$0{,}65 \pm 0{,}033$	$0{,}63 \pm 0{,}032$	$0{,}64 \pm 0{,}032$	$0{,}63 \pm 0{,}032$
p	$p \succ 0{,}05$				
SM_3	$1{,}31 \pm 0{,}062$	$1{,}35 \pm 0{,}066$	$1{,}46 \pm 0{,}072$	$1{,}39 \pm 0{,}065$	$1{,}38 \pm 0{,}063$
p	$p \succ 0{,}05$				
SM_4	$0{,}92 \pm 0{,}048$	$1{,}06 \pm 0{,}057$	$1{,}11 \pm 0{,}064$	$1{,}13 \pm 0{,}065$	$1{,}14 \pm 0{,}066$
p	$p \succ 0{,}05$				

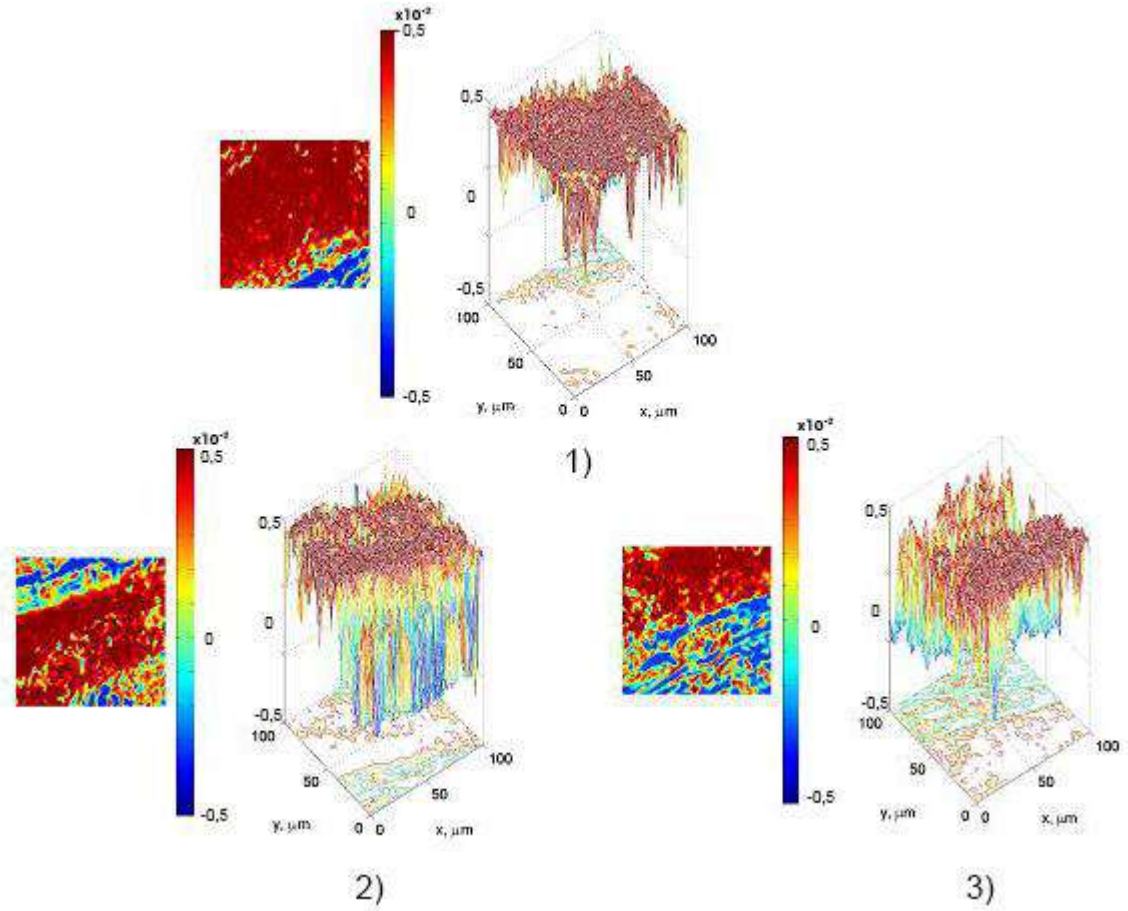

Fig. 2. Maps ((1), (2), (3)) and coordinate distributions ((4), (5), (6)) of the MMI value of linear birefringence (x40) of histological brain sections from the control group ((1), (4)), research groups with different age of damage (6 hours - (2), (5)) and (18 hours - (3), (6)).

Table 2 Time dynamics of changes in the statistical moments of the 1st - 4th orders characterizing the distributions of the MMI value of linear birefringence (40x) of histological brain sections

T, hours	**2**	**4**	**6**	**12**	**18**
SM_1 x10^{-1}	$0,34 \pm 0,014$	$0,25 \pm 0,011$	$0,23 \pm 0,012$	$0,22 \pm 0,012$	$0,23 \pm 0,013$
p	$p \prec 0,05$		$p \succ 0,05$		
SM_2 x10^{-1}	$1,39 \pm 0,061$	$1,08 \pm 0,048$	$0,89 \pm 0,036$	$0,84 \pm 0,034$	$0,81 \pm 0,035$
p	$p \prec 0,05$			$p \succ 0,05$	
SM_3	$0,29 \pm 0,013$	$0,41 \pm 0,018$	$0,55 \pm 0,023$	$0,79 \pm 0,034$	$1,03 \pm 0,048$
p	$p \prec 0,05$				
SM_4	$0,13 \pm 0,06$	$0,24 \pm 0,011$	$0,36 \pm 0,016$	$0,61 \pm 0,027$	$0,84 \pm 0,038$
p	$p \prec 0,05$				
T, hours	**24**	**48**	**72**	**96**	**120**
SM_1 x10^{-1}	$0.22 \pm 0,013$	$0,24 \pm 0,012$	$0,22 \pm 0,011$	$0,23 \pm 0,012$	$0,22 \pm 0,011$

p	$p \succ 0{,}05$				
SM_2 x10^{-1}	$0{,}83 \pm 0{,}045$	$0{,}85 \pm 0{,}043$	$0{,}83 \pm 0{,}042$	$0{,}84 \pm 0{,}042$	$0{,}81 \pm 0{,}042$
p	$p \succ 0{,}05$				
SM_3	$1{,}24 \pm 0{,}11$	$1{,}28 \pm 0{,}14$	$1{,}33 \pm 0{,}17$	$1{,}39 \pm 0{,}15$	$1{,}44 \pm 0{,}12$
p	$p \prec 0{,}05$	$p \succ 0{,}05$			
SM_4	$1{,}07 \pm 0{,}094$	$1{,}11 \pm 0{,}12$	$1{,}15 \pm 0{,}13$	$1{,}19 \pm 0{,}15$	$1{,}14 \pm 0{,}11$
p	$p \prec 0{,}05$	$p \succ 0{,}05$			

The dynamic ranges, as well as the diagnostic sensitivity to the age of brain damage, of statistical moments of the 1st-4th orders with the following time intervals of linear and statistically significant changes in eigenvalues have been established:

- 1st order statistical moment (average) – 6 hours and 0,09;
- 2nd order statistical moment (dispersion) – 12 hours and 0,05;
- 3rd order statistical moment (skewness) – 24 hours and 0,74;
- 4th order statistical moment (kurtosis) – 24 hours and 0,71.

From the analysis of the data obtained, an increase (up to 4) in the number of diagnostic-sensitive statistical parameters (average, dispersion, skewness and kurtosis of histograms of the distributions of MMI of the degree of crystallization of brain tissue) and the duration of the range of linear change in their magnitude from the age of damage were established..

4. DIFFERENTIAL HISTOLOGICAL DIAGNOSIS OF THE AGE OF THE FORMATION OF INJURIES OF HUMAN INTERNAL ORGANS BY MAPPING THE MUELLER-MATRIX INVARIANT OF CIRCULAR BIREFRINGENCE

Two-dimensional maps of the Mueller-matrix invariant of circular birefringence of histological sections of the brain ((1) - (3)) and histograms ((4) - (6)) of the distribution of its magnitude are shown in Fig. 3.

Comparison of the digital histology data of the degree of crystallization of the brain substance (Fig. 2) also revealed the topographic structure (Fig. 3, fragments (4) - (6)) of the distributions of the MMI CB value and coordinate heterogeneity (Fig. 3, fragments (1) - (3)).

It was also found that with an increase in the age of damage, the average and dispersion of the MMI CB decrease (Fig. 3, fragments (5) and (6)), and the skewness and kurtosis of such distributions, on the contrary, increase - Table 3.

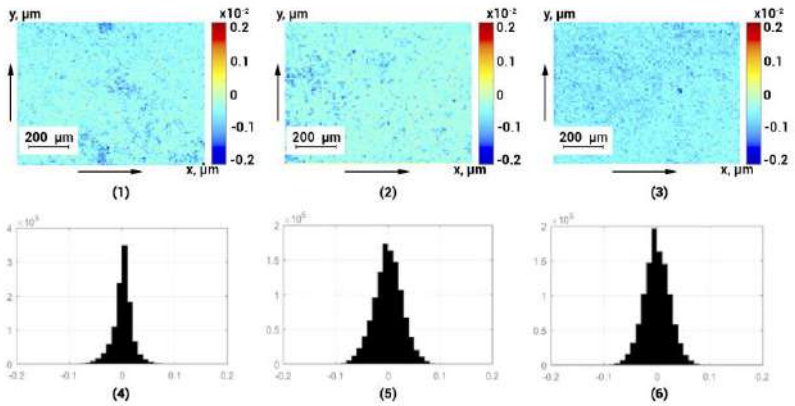

Fig. 3. Maps ((1), (2), (3)) and histograms ((4), (5), (6)) of the distributions of the MMI value of circular birefringence (x4) of histological sections of the brain of the deceased from the control group ((1), (4)), research groups with different duration of damage (6 hours - (2), (5)) and (18 hours - (3), (6)).

Table 3 Time dynamics of changes in the statistical moments of the 1st - 4th orders characterizing the distributions of the MMI value of circular birefringence (4x) of histological sections of the brain

T, hours	**2**	**4**	**6**	**12**	**18**
SM_1 x10^{-1}	$0{,}19 \pm 0{,}009$	$0{,}17 \pm 0{,}008$	$0{,}16 \pm 0{,}008$	$0{,}15 \pm 0{,}007$	$0{,}13 \pm 0{,}006$
p	$p \succ 0{,}05$				
SM_2 x10^{-1}	$0{,}17 \pm 0{,}007$	$0{,}105 \pm 0{,}004$	$0{,}09 \pm 0{,}005$	$0{,}08 \pm 0{,}004$	$0{,}09 \pm 0{,}005$
p	$p \prec 0{,}05$		$p \succ 0{,}05$		
SM_3	$0{,}59 \pm 0{,}029$	$0{,}71 \pm 0{,}032$	$0{,}83 \pm 0{,}039$	$1{,}09 \pm 0{,}042$	$1{,}33 \pm 0{,}058$
p	$p \prec 0{,}05$				
SM_4	$0{,}71 \pm 0{,}028$	$0{,}97 \pm 0{,}043$	$1{,}22 \pm 0{,}056$	$1{,}73 \pm 0{,}082$	$1{,}98 \pm 0{,}091$
p	$p \prec 0{,}05$				
T, hours	**24**	**48**	**72**	**96**	**120**
SM_1 x10^{-1}	$0.13 \pm 0{,}009$	$0{,}14 \pm 0{,}008$	$0{,}12 \pm 0{,}007$	$0{,}11 \pm 0{,}008$	$0{,}12 \pm 0{,}007$
p	$p \succ 0{,}05$				
SM_2 x10^{-1}	$0{,}08 \pm 0{,}005$	$0{,}065 \pm 0{,}003$	$0{,}063 \pm 0{,}003$	$0{,}064 \pm 0{,}003$	$0{,}063 \pm 0{,}003$
p	$p \succ 0{,}05$				
SM_3	$1{,}31 \pm 0{,}062$	$1{,}35 \pm 0{,}066$	$1{,}46 \pm 0{,}072$	$1{,}39 \pm 0{,}065$	$1{,}38 \pm 0{,}063$
p	$p \succ 0{,}05$				
SM_4	$1{,}92 \pm 0{,}098$	$2{,}06 \pm 0{,}097$	$2{,}11 \pm 0{,}11$	$2{,}13 \pm 0{,}12$	$2{,}14 \pm 0{,}12$
p	$p \succ 0{,}05$				

An increase in the number of diagnostic parameters of this method by Mueller-matrix microscopy in comparison with the method of detecting the degree of crystallization of the brain substance is shown. Along with the intervals of linear change in the statistical moments of higher orders (18 hours, dynamic range 0.74 and 1.26), a linear change in the dispersion characterizing the spread of the MMI CB value was revealed over a time interval of up to 4 hours with a dynamic range of 0.055.

The results of the azimuthal-invariant Mueller matrix mapping of large-scale (40x) maps of the MMI CB of histological brain sections are presented in a series of fragments in Fig. 4.

Comparative analysis of the obtained data (Fig. 4) with small-scale maps of MMI CB (Fig. 3) revealed an increase in the range of variation in the magnitude of fluctuations in the values of optical activity of molecular complexes of brain samples, - Table 4.

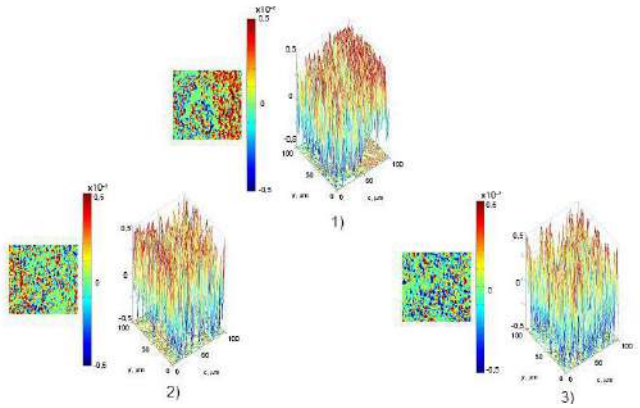

Fig. 4. Maps ((1), (2), (3)) and coordinate distributions ((4), (5), (6)) of the magnitude of MMI circular birefringence (x40) histological sections of the brain of the deceased from the control group ((1), (4)), research groups with different age of damage (6 hours - (2), (5)) and (18 hours - (3), (6)).

Table 4 Time dynamics of changes in the statistical moments of the 1st - 4th orders characterizing the distribution of MMI circular birefringence (40x) of brain sections

T, hours	**2**	**4**	**6**	**12**	**18**
SM_1 x10^{-1}	$0{,}16 \pm 0{,}07$	$0{,}11 \pm 0{,}004$	$0{,}09 \pm 0{,}005$	$0{,}08 \pm 0{,}007$	$0{,}085 \pm 0{,}006$
p	$p \succ 0{,}05$				
SM_2 x10^{-1}	$0{,}14 \pm 0{,}007$	$0{,}095 \pm 0{,}004$	$0{,}069 \pm 0{,}003$	$0{,}068 \pm 0{,}004$	$0{,}069 \pm 0{,}005$
p	$p \prec 0{,}05$			$p \succ 0{,}05$	
SM_3	$0{,}65 \pm 0{,}029$	$0{,}79 \pm 0{,}032$	$0{,}93 \pm 0{,}043$	$1{,}29 \pm 0{,}054$	$1{,}57 \pm 0{,}065$
p	$p \prec 0{,}05$				
SM_4	$0{,}87 \pm 0{,}038$	$1{,}17 \pm 0{,}053$	$1{,}49 \pm 0{,}065$	$2{,}07 \pm 0{,}098$	$2{,}68 \pm 0{,}14$
p	$p \prec 0{,}05$				
T, hours	**24**	**48**	**72**	**96**	**120**
SM_1 x10^{-1}	$0.068 \pm 0{,}003$	$0{,}049 \pm 0{,}002$	$0{,}037 \pm 0{,}001$	$0{,}034 \pm 0{,}002$	$0{,}029 \pm 0{,}001$
p	$p \succ 0{,}05$				
SM_2 x10^{-1}	$0{,}068 \pm 0{,}005$	$0{,}065 \pm 0{,}003$	$0{,}063 \pm 0{,}002$	$0{,}064 \pm 0{,}002$	$0{,}063 \pm 0{,}002$
p	$p \succ 0{,}05$				
SM_3	$1{,}85 \pm 0{,}17$	$1{,}89 \pm 0{,}18$	$1{,}96 \pm 0{,}17$	$1{,}99 \pm 0{,}95$	$1{,}93 \pm 0{,}16$
p	$p \prec 0{,}05$	$p \succ 0{,}05$			
SM_4	$3{,}02 \pm 0{,}26$	$3{,}11 \pm 0{,}29$	$3{,}13 \pm 0{,}33$	$3{,}19 \pm 0{,}32$	$3{,}14 \pm 0{,}31$
p	$p \prec 0{,}05$	$p \succ 0{,}05$			

The growth (all statistical moments of the 1st - 4th orders) of the number of diagnostic-sensitive parameters (average, dispersion, skewness and kurtosis of histograms of distributions of MMI CB of brain tissue) and the duration of the range of statistically significant ($p \prec 0{,}05$) linear changes in their magnitude from the age of damage was established:

- 1st order statistical moment (average) – 6 hours and 0,05;
- 2nd order statistical moment (dispersion) – 12 hours and 0,075;

- 3rd order statistical moment (skewness) – 24 hours and 1,2;
- 4th order statistical moment (kurtosis) – 24 hours and 2,15.

5. TIME INTERVALS AND ACCURACY OF DIGITAL HISTOLOGICAL DETERMINATION OF THE AGE OF DAMAGE BY THE METHODS OF AZIMUTHAL-INVARIANT MUELLER-MATRIX MAPPING

Table 5 Time intervals and accuracy of the method of polarization mapping of MMI maps of linear birefringence

Brain				
Statistical moments	Interval, hours		Accuracy, min.	
Magnification	4x	40x	4x	40x
Average,	_	4	_	70
Dispersion,	6	6	65	60
Skewness,	18	24	50	40
Kurtosis,	18	24	50	40
Myocardium				
Statistical moments	Interval, hours		Accuracy, min.	
Magnification	4x	40x	4x	40x
Average,	_	4	_	70
Dispersion,	6	6	65	60
Skewness,	18	24	50	40
Kurtosis,	18	24	50	40
Liver				
Statistical moments	Interval, hours		Accuracy, min.	
Magnification	4x	40x	4x	40x
Average,	_	4	_	70
Dispersion,	6	6	65	60
Skewness,	18	24	55	45
Kurtosis,	18	24	55	45
Lung tissue				
Statistical moments	Interval, hours		Accuracy, min.	
Magnification	4x	40x	4x	40x
Average,	_	4	_	70
Dispersion,	6	6	65	60
Skewness,	18	24	55	45
Kurtosis,	18	24	55	45
Kidney				
Statistical moments	Interval, hours		Accuracy, min.	
Magnification	4x	40x	4x	40x
Average,	_	4	_	70
Dispersion,	6	6	65	60
Skewness,	18	24	50	40
Kurtosis,	18	24	50	40

Table 6 Time intervals and accuracy of the method of polarization mapping of MMI maps of circular birefringence

Brain				
Statistical moments	Interval, hours		Accuracy, min.	
Magnification	4x	40x	4x	40x
Average,	_	4	_	65
Dispersion,	6	6	60	55

Skewness,	18	24	45	35
Kurtosis,	18	24	45	35
Myocardium				
Statistical moments	Interval, hours		Accuracy, min.	
Magnification	4x	40x	4x	40x
Average,	_	4	_	65
Dispersion,	6	6	60	55
Skewness,	18	24	45	35
Kurtosis,	18	24	45	35
Liver				
Statistical moments	Interval, hours		Accuracy, min.	
Magnification	4x	40x	4x	40x
Average,	_	4	_	65
Dispersion,	6	6	60	55
Skewness,	18	24	50	40
Kurtosis,	18	24	50	40
Lung tissue				
Statistical moments	Interval, hours		Accuracy, min.	
Magnification	4x	40x	4x	40x
Average,	_	4	_	65
Dispersion,	6	6	60	55
Skewness,	18	24	50	40
Kurtosis,	18	24	50	40
Kidney				
Statistical moments	Interval, hours		Accuracy, min.	
Magnification	4x	40x	4x	40x
Average,	_	4	_	65
Dispersion,	6	6	60	55
Skewness,	18	24	45	35
Kurtosis,	18	24	45	35

CONCLUSIONS

1. By using a new digital histological technique based on azimuthal-invariant Muller-matrix mapping of optically anisotropic molecular fluorophores of samples of human internal organs with different periods of damage (brain, liver, kidney, as well as myocardium and lung tissue), changes in the morphological and biochemical structure have been studied for the first time on interval from 1 hour up to 120 hours..

2. For the first time, the main interrelationships between temporal changes in the statistical structure of maps of Mueller-matrix invariants of linear (degree of crystallization) and circular (optical activity) birefringence of molecular fluorophores in histological sections of human internal organs and variations in the magnitude of statistical moments of the 1st - 4th orders that characterize them have been revealed - with an increase in the age of damage, the value of the average and dispersion decreases, skewness and kurtosis, on the contrary, increase.

3. Diagnostic-sensitive parameters have been established - the time ranges of linear changes in the variations in the magnitude of the statistical indicators of the Mueller-matrix digital histology methods and the accuracy of determining the duration of damage:

3.1. MMI maps of crystallization degree (4x):

- dispersion – 6 h.;
- skewness – 18 h.;
- kurtosis – 18 h.;

- accuracy 60 min. – 70 min.

3.2. MMI maps of crystallization degree (40x):

- average – 4 h.;
- dispersion – 6 h.;
- skewness – 24 h.;
- kurtosis – 24 h..;
- accuracy – 55 min. – 60 min.

3.3. MMI optical activity maps (4x):

- dispersion – 6 h.;
- skewness – 18 h.;
- kurtosis – 18 h.;
- accuracy - 70 min. – 80 min.

3.4. MMI optical activity maps (40x):

- average – 4 h.;
- dispersion – 6 h.;
- skewness– 24 h.;
- kurtosis– 24 h.;
- accuracy – 65 min. – 75 min.

FUNDING

Current research supported by the National Research Foundation of Ukraine (Project 2020.02/0061)

REFERENCES

[1] Wang X. Propagation of polarized light in birefringent turbid media: a Monte Carlo study / X. Wang, L.-H. Wang // J. Biomed. Opt. – 2002. – Vol. 7. – P. 279-290.

[2] Tuchin V. V. Handbook of optical biomedical diagnostics / V. V. Tuchin. – Bellingham : SPIE Press, 2002. – 1110 p.

[3] Yao G. Two-dimensional depth-resolved Mueller matrix characterization of biological tissue by optical coherence tomography / G. Yao, L. V. Wang // Opt. Lett. – 1999. – V. 24. – P. 537-539.

[4] Tower T. T. Alignment Maps of Tissues: I. Microscopic Elliptical Polarimetry / T. T. Tower, R. T. Tranquillo // Biophys. J. – 2001. – Vol. 81. – P. 2954-2963.

[5] Lu S. Interpretation of Mueller matrices based on polar decomposition / S. Lu, R. A. Chipman // J. Opt. Soc. Am. A. – 1996. – Vol. 13. – P. 1106-1113.

[6] Ushenko, V.A., Hogan, B.T., Dubolazov, A., Piavchenko, G., Kuznetsov, S.L., Ushenko, A.G., Ushenko, Y.O., Gorsky, M., Bykov, A., Meglinski, I. 3D Mueller matrix mapping of layered distributions of depolarisation degree for analysis of prostate adenoma and carcinoma diffuse tissues (2021) Scientific Reports, 11 (1), 5162.

[7] Ushenko, V.A., Hogan, B.T., Dubolazov, A., Grechina, A.V., Boronikhina, T.V., Gorsky, M., Ushenko, A.G., Ushenko, Y.O., Bykov, A., Meglinski, I. Embossed topographic depolarisation maps of biological tissues with different morphological structures (2021) Scientific Reports, 11 (1), № 3871.

[8] Ushenko, V.O., Trifonyuk, L., Ushenko, Y.A., Dubolazov, O.V., Gorsky, M.P., Ushenko, A.G. Polarization singularity analysis of Mueller-matrix invariants of optical anisotropy of biological tissues samples in cancer diagnostics (2021) Journal of Optics (United Kingdom), 23 (6), статья № 064004.

[9] Meglinski, I., Trifonyuk, L., Bachinsky, V., Vanchulyak, O., Bodnar, B., Sidor, M., Dubolazov, O., Ushenko, A., Ushenko, Y., Soltys, I.V., Bykov, A., Hogan, B., Novikova, T. Polarization Correlometry of Microscopic Images of Polycrystalline Networks Biological Layer (2021) SpringerBriefs in Applied Sciences and Technology, pp. 61-73.

[10] Meglinski, I., Trifonyuk, L., Bachinsky, V., Vanchulyak, O., Bodnar, B., Sidor, M., Dubolazov, O., Ushenko, A., Ushenko, Y., Soltys, I.V., Bykov, A., Hogan, B., Novikova, T. Scale-Selective and Spatial-Frequency Correlometry of Polarization-Inhomogeneous Field (2021) SpringerBriefs in Applied Sciences and Technology, pp. 33-59.

[11] Meglinski, I., Trifonyuk, L., Bachinsky, V., Vanchulyak, O., Bodnar, B., Sidor, M., Dubolazov, O., Ushenko, A., Ushenko, Y., Soltys, I.V., Bykov, A., Hogan, B., Novikova, T. Multifunctional Stokes Correlometry of Biological Layers (2021) SpringerBriefs in Applied Sciences and Technology, pp. 75-96.

[12] Meglinski, I., Trifonyuk, L., Bachinsky, V., Vanchulyak, O., Bodnar, B., Sidor, M., Dubolazov, O., Ushenko, A., Ushenko, Y., Soltys, I.V., Bykov, A., Hogan, B., Novikova, T. Methods and Means of Polarization Correlation of

Fields of Laser Radiation Scattered by Biological Tissues (2021) SpringerBriefs in Applied Sciences and Technology, pp. 1-15.

[13] Meglinski, I., Trifonyuk, L., Bachinsky, V., Vanchulyak, O., Bodnar, B., Sidor, M., Dubolazov, O., Ushenko, A., Ushenko, Y., Soltys, I.V., Bykov, A., Hogan, B., Novikova, T. Materials and Methods (2021) SpringerBriefs in Applied Sciences and Technology, pp. 17-31.

[14] Angelsky, O.V., Ushenko, Y.A., Dubolazov, A.V., Telenha, O.Yu. The interconnection between the coordinate distribution of mueller-matrixes images characteristic values of biological liquid crystals net and the pathological changes of human tissues (2010) Advances in Optical Technologies, 130659

[15] Trifonyuk, L., Sdobnov, A., Baranowski, W., Ushenko, V., Olar, O., Dubolazov, A., Pidkamin, L., Sidor, M., Vanchuliak, O., Motrich, A., Gorsky, M., Meglinski, I Differential Mueller matrix imaging of partially depolarizing optically anisotropic biological tissues (2020) Lasers in Medical Science, 35 (4), pp. 877-891.

[16] Borovkova, M., Trifonyuk, L., Ushenko, V., Dubolazov, O., Vanchulyak, O., Bodnar, G., Ushenko, Y., Olar, O., Ushenko, O., Sakhnovskiy, M., Bykov, A., Meglinski, I. Mueller-matrix-based polarization imaging and quantitative assessment of optically anisotropic polycrystalline networks (2019) PLoS ONE, 14 (5), e0214494 .

[17] P. Wang, X. Zhang, Y. Xiang, F. Shi, M. Gavryliak, and J. Xu, "Random laser with superscatterers at designable wavelengths," Opt. Express 23, 24407-24415.

[18] Angelsky, O.V., Zenkova, C.Y., Gorsky, M.P., Gorodyńska, N.V. Feasibility of estimating the degree of coherence of waves at the near field (2009) Applied Optics, 48 (15), pp. 2784-2788

[19] Angelsky, O.V., Bekshaev, A.Y., Hanson, S.G., Zenkova, C.Y., Mokhun, I.I., Jun, Z. Structured Light: Ideas and Concepts (2020) Frontiers in Physics, 8, 114

[20] Valery V. Tuchin, Lihong Wang, Dmitry A. Zimnyakov, "Optical Polarization in Biomedical Applications," in Biological and Medical Physics, Biomedical Engineering, Springer-Verlag Berlin Heidelberg, p.281, 2006. DOI 10.1007/978-3-540-45321-5.

[21] N. Ghosh and I. A. Vitkin, "Tissue polarimetry: concepts, challenges, applications and outlook," J. Biomed. Opt. 16, 110801 (2011).

[22] N. Ghosh, M. F. G. Wood, and I. A. Vitkin, "Polarized light assessment of complex turbid media such as biological tissues via Mueller matrix decomposition," in Handbook of Photonics for Biomedical Science, V.V. Tuchin, Ed., pp. 253–282, CRC Press, Taylor & Francis Group, London (2010).

[23] Vitkin, N.Ghosh, and A. de Martino, "Tissue polarimetry" in Photonics: Scientific Foundations, Technology and Applications, D.L. Andrews, Ed., Vol. IV, pp. 239–321, John Wiley & Sons, Inc., Hoboken, New Jersey (2015).

[24] Angelsky, O.V., Bekshaev, A.Y., Dragan, G.S., Maksimyak, P.P., Zenkova, C.Y., Zheng, J. Structured Light Control and Diagnostics Using Optical Crystals (2021) Frontiers in Physics, 9,715045.

[25] Angelsky, O.V., Maksimyak, P.P. Optical diagnostics of slightly rough surfaces (1992) Applied Optics, 31 (1), pp. 140-143.

[26] Angelsky, O.V., Zenkova, C.Y., Hanson, S.G., Zheng, J. Extraordinary Manifestation of Evanescent Wave in Biomedical Application (2020) Frontiers in Physics, 8, 159.